Effects of Immunoproteasome Inhibition on Adenovirus Pathogenesis

Danielle Malitz

University of Michigan - Class of 2015

Undergraduate Program in Biology - Microbiology Honors

TABLE OF CONTENTS

ABSTRACT

Pediatric myocarditis is frequently caused by adenoviruses. However, little is currently known about adenoviral myocarditis infection and its viral pathogenesis. One such virus that can cause viral myocarditis are human adenoviruses (HAdV). The use of mouse adenovirus type 1 (MAV-1) in the lab allows us to investigate the pathogenesis of an adenovirus in its natural host, which can't be done with HAdV due to the species specific nature of adenoviruses.The immunoproteasome (IP) is a host factor that contributes to the generation of peptides presented by MHC class I molecules to CD8 T cells of the adaptive immune system. IP activity also plays a significant role in the activation of inflammatory responses, so it is thereby likely that the IP contributes to pathology in viral myocarditis. The data presented in this paper suggest that the IP may contribute to the regulation of proinflammatory cytokine production during MAV-1 myocarditis. Achieving a better understanding of the IP and its role in adenovirus infection is one of the first steps towards improving treatments and vaccines for viral infection.

INTRODUCTION

Acute myocarditis, or inflammation of the heart muscle, is a significant cause of morbidity and mortality in children (McCarthy et al., 2015). Viruses, including HAdV, are often identified as causes of acute myocarditis (McCarthy et al., 2015). Cardiac dysfunction due to HAdV myocarditis has frequently been found to be more severe in neonates and infants than in older adult patients (Amabile et al., 2006). Currently, very little is known about virus or host factors that contribute to adenovirus myocarditis. In order to develop appropriate strategies for prevention or treatment, the factors that contribute to disease manifestation must be identified. We have established a mouse model of HAdV myocarditis using MAV-1, which has

allowed us to study both the virus and host-associated factors that contribute to cardiac dysfunction caused by adenovirus infection.

During viral infection, the host immune response causes both a decrease in viral replication and host tissue damage if the response is not regulated properly. One of the major intracellular degradation pathways involved in the host immune response is the ubiquitin-proteasome system (UPS), which is emerging as an important regulator of viral replication and host inflammation (McCarthy et al., 2014). Enzymes involved in protein ubiquitination/deubiquitination are upregulated following infection by a variety of viruses, and many viruses encode proteins that directly influence pathways involved in the UPS (Rock et al., 1994). A specialized type of proteasome - the IP - has altered peptide cleavage properties, playing a key role during viral infection via proinflammatory cytokine production, activation of the NF-κB pathway, and activation of CD8 T cells (Groettrup et al., 1997). CD8 T cell activation occurs when T cells recognize peptides cleaved by the IP and presented by MHC class I (Groettrup et al., 1997). Antigen-presenting immune cells express a high basal level of IPs (McCarthy et al., 2014). The IP is also induced in nonimmune cells by inflammation (particularly due to IFN-ɣ cytokine release) (Shin et al., 2006). Inhibition of host IP function can affect viral pathogenesis, altering both viral replication and virus-induced inflammatory responses (McCarthy et al., 2014). However, not much is known about ways in which IP function contributes to adenovirus pathogenesis. Recently, it has been shown that there is a substantial induction of IFN-ɣ expression in the hearts of MAV-1 infected neonatal mice (McCarthy et al., 2015). Recent work in our lab demonstrated upregulation of IP subunit expression in the hearts of infected mice, and this corresponded to increased IP activity at 11 days post-infection (dpi) (Mary McCarthy, unpublished data).

The goal of this project was to use MAV-1 to study the impact of IP function on adenovirus pathogenesis. This was accomplished by studying the differences in the outcomes of viral infection between LMP7 homozygote wild type, heterozygote, and homozygote knockout mice. The assembly of the IP is cooperative, meaning that the immunosubunits (β1i, β2i, and β5i) interact with each other, ultimately promoting the formation of the IP containing all three subunits (McCarthy et al., 2014). The β5i subunit, also known as LMP7, is absolutely required for catalytic activity, as it promotes the necessary maturation of β1i and β2i (Griffin et al., 1998). Additionally, β5i is the only immunosubunit that can be incorporated into the complex without the others (Griffin et al., 1998). LMP7 knockout mice lack the ability to make the β5i subunit, rendering them deficient in IP activity.

A significant objective of research in the Weinberg Laboratory is to understand interactions between adenoviruses and host immune responses in the context of adenovirus myocarditis. This thesis will contribute to this larger picture by providing specific data on how IP function influences adenovirus replication and adenovirus-induced inflammation in the host. I hypothesized that IP inhibition would suppress virus-induced inflammation. The results of my work provide a deeper understanding of how IP function affects viral pathogenesis, and offer insight for improving efforts to develop vaccines or therapies for people with myocarditis caused by adenoviruses and other viral pathogens.

METHODS

LMP7 KO Mice

All work was approved by the University of Michigan Committee on Use and Care of Animals. Litters of homozygote wild type ($LMP7^{+/+}$), heterozygote ($LMP7^{+/-}$), and homozygote knockout

(LMP7$^{-/-}$) mice were obtained by breeding heterozygote to heterozygote mice in-house. All mice were maintained under specific-pathogen-free conditions.

Virus and Infections

Neonates (7 days old) were manually restrained and infected intranasally (i.n.) with 10^5 plaque-forming units of MAV-1 in 10 µl of sterile phosphate-buffered saline (PBS). Control mice were mock infected i.n. with conditioned medium at an equivalent dilution in sterile PBS. Mice were euthanized by pentobarbital overdose. Blood was collected from the posterior vena cava of euthanized neonates and incubated on ice for approximately 30 m. Samples were centrifuged in a tabletop microcentrifuge at 13,000 × g for 10 min at 4°C. Serum was transferred to a new labeled microcentrifuge tube and stored at −80°C. After blood collection, hearts were harvested, snap-frozen in dry ice, and stored at −80°C. Approximately one-third of each heart was homogenized in TRIzol (Invitrogen) using sterile glass beads in a mini-Beadbeater (Biospec Products) for 30 s. RNA and DNA were isolated from the homogenates according to the manufacturer's protocol.

Real-time PCR Analysis of Gene Expression

Cytokine gene expression was quantified using reverse transcriptase quantitative real-time PCR (RT-qPCR). 2.5 µg of RNA was used and reverse transcribed using Moloney murine leukemia virus (MMLV) reverse transcriptase in 20-µl reaction mixtures according to the manufacturer's (Invitrogen) instructions. Once the cDNA product was obtained, 30 µl of water was added to bring the total volume to 50 µl. cDNA was then amplified using duplexed gene expression assays for mouse CCL5 and GAPDH (Applied Biosystems). Five microliters of cDNA was added to reaction mixtures containing TaqMan universal PCR mix and 1.25 µl each of 20X gene expression assay mixtures for the target cytokine and GAPDH. Primers

from Applied Biosystems were used to detect Chemokine (C-C motif) ligand 5 (CCL5). A second qPCR method was used to to detect interferon gamma (IFN-ɣ), tumor necrosis factor alpha (TNF-α), GAPDH, interleukin 6 (IL-6), interleukin 1 beta (IL-1β), beta 1i (β1i), beta 2i (β2i), and beta 5i (β5i) (Table 1). Five microliters of cDNA was added to reaction mixtures containing Power SYBR green PCR master mix and 0.5 µl of each specific forward and reverse primer. In both methods, RT-qPCR analysis consisted of 40 cycles of 15 s at 90 °C and 60 s at 60 °C. Quantification of each gene of interest was normalized to GAPDH and expressed in arbitrary units (A.U.) as $2^{-\Delta CT}$. CT is the threshold cycle, and the ΔCT value is obtained by subtracting the CT(GAPDH) value from the CT(target gene) value (ΔCT=CT(target gene)-CT(GAPDH)).

Analysis of Viral Loads by PCR

MAV-1 viral loads were measured in hearts using quantitative real-time PCR (qPCR). Five microliters of extracted DNA was added to reaction mixtures containing TaqMan II universal PCR mix with uracil N-glycosylase (UNG) (Applied Biosystems), forward and reverse primers (detect a 59-bp region of the MAV-1 E1A gene, each at a 200 nM final concentration), and probe (20 nM final concentration) in a 25-µl reaction volume. Analysis on an ABI Prism 7300 machine (Applied Biosystems) consisted of 40 cycles of 15 s at 90°C and 60 s at 60°C. Standard curves generated using known amounts of plasmid containing the MAV-1 E1A gene were used to convert threshold cycle values for experimental samples to copy numbers of E1A DNA. Results were standardized to the nanogram amount of input DNA. Each sample was assayed in triplicate.

Histology

Hearts were fixed in 10% formalin and embedded in paraffin. Five-micrometer sections were stained with hematoxylin and eosin to evaluate cellular infiltrates. Separate sections were stained with CD3 antibody (Thermo Scientific). CD3+ cells were quantified at a magnification of 40X, using the average from at least 20 independent fields per sample. Results are expressed as the number of CD3+ cells per high-power field (HPF). Images were assembled using Adobe Illustrator (Adobe Systems). To quantify cellular inflammation in the hearts, slides were examined in a blinded fashion to determine a pathology index score for the size and intensity of cellular infiltrate and the extent of pathological involvement in the heart (Table 2).

Determination of Serum Cardiac Troponin Levels

Cardiac troponin I (cTnI) concentrations were measured using the Ultra Sensitive Mouse Cardiac Troponin-I ELISA kit (Life Diagnostics) according to the manufacturer's instructions. Samples were assayed in duplicate.

Statistics

Analysis for statistical significance was conducted using Prism 6 for Macintosh (GraphPad Software, Inc.). Differences between groups at multiple time points were analyzed using two-way ANOVA followed by Bonferroni's multiple-comparison tests. Differences in log-transformed viral loads for viral loads data between groups at a given time point were analyzed using the Mann-Whitney test. P values of less than 0.05 were considered statistically significant.

RESULTS

Immunoproteasome Subunit Expression in LMP7$^{-/-}$ Mice

β5i, β1i, and β2i gene expression was upregulated in all infected LMP7$^{+/+}$ mice relative to mock-infected mice. To verify that β5i expression was absent in LMP7$^{-/-}$ mice, RT-qPCR was used to quantify β5i mRNA levels in the hearts of mock infected and infected mice (Fig. 1A). As expected, LMP7$^{+/+}$ mice had the highest level of β5i gene expression, while β5i expression was essentially absent in LMP7$^{-/-}$ mice (Fig. 1A). There was a statistically significant difference when β5i expression in infected LMP7$^{+/+}$, LMP7$^{+/-,}$ and LMP7$^{-/-}$ mice were compared (any β5i qPCR expression present in the LMP7$^{-/-}$ mice was likely due to nonspecific background). LMP7$^{+/-}$ mice expressed β5i at a level that fell between the LMP7$^{+/+}$ and LMP7$^{-/-}$ mice. It was important to confirm that the genetic modifications did, in fact, have the desired effect on β5i expression.

To verify that there was no compensatory upregulation of β1i or β2i when β5i was absent, β1i and β2i expression was also measured using RT-qPCR (Fig. 1B,C). β1i and β2i followed a trend similar to β5i, in that the gene expression of each subunit was slightly decreased in LMP7$^{+/-}$ and LMP7$^{-/-}$ mice compared to LMP7$^{+/+}$ mice. However, unlike with β5i, these differences in β1i and β2i expression were not statistically significant. These results confirmed that there was no compensatory upregulation of β1i and β2i gene expression in response to β5i deficiency.

Effect of Immunoproteasome Deficiency on Virus-Induced Inflammation

To determine the effect of IP deficiency on virus-induced expression of proinflammatory cytokines, IFN-ɣ mRNA levels were measured in the hearts of mock infected and infected mice (Fig. 2A). IFN-ɣ was expressed at a much higher level in infected mice than

mock-infected mice (Fig. 2A). However, the levels of IFN-ɣ gene expression were similar among all three LMP7 genotypes (Fig. 2A). This suggests that there was no significant effect of β5i deficiency on IFN-ɣ expression. TNF-α followed a trend similar to IFN-ɣ, with no significant differences between LMP7 genotypes in TNF-α gene expression (Fig. 2B). Virus-induced IL-1β gene expression followed a similar trend to the immunosubunits, with the lowest level of expression in LMP7$^{-/-}$ mice (Fig. 2C). There was no significant difference in gene expression between groups. This result may have been due to the relatively small number of mice in some groups. Overall, the data shown suggest a correlation between the IP and IL-1β, where decreased IP activity was associated with less IL-1β expression in the heart (Fig. 2C).

To determine the effect of IP deficiency on other components of the immune response to MAV-1 infection, we measured the expression of CCL5 in the hearts. As expected, mock-infected mice expressed the lowest levels of CCL5 overall. However, contrary to what was seen with IL-1β, virus-induced CCL5 expression was greater in LMP7$^{+/-}$ and LMP7$^{-/-}$ mice than in LMP7$^{+/+}$ mice (Fig. 2D).

Effect of LMP7 Deficiency on Inflammatory Infiltrates in Infected Hearts

To further assess the inflammatory response to MAV-1 infection in the heart, the histological appearance of heart tissue was evaluated. LMP7$^{-/-}$ mice had fewer inflammatory cell infiltrates than the mice that were wild type for the β5i gene. A greater number of focal accumulations of inflammatory cells were present in the wild type mice, and these larger foci were found in many areas across the tissue samples (Fig. 3A). Inflammation was less severe in LMP7$^{-/-}$ mice than in LMP7$^{+/+}$ mice (Fig. 3B). When quantified, virus-induced cardiac pathology was less severe in LMP7$^{-/-}$ mice than in LMP7$^{+/+}$ mice (Fig. 3C).

Immunohistochemistry was used to evaluate and quantify recruitment of inflammatory cells to hearts following MAV-1 infection of neonates at 9 dpi (Fig. 3D,E,F). There was no significant difference between the number of $CD3^+$ T lymphocytes detected in the hearts of $LMP7^{-/-}$ mice compared to $LMP7^{+/+}$ mice (Fig. 3F).

Histological evaluation suggested that MAV-1 infection induces cardiac damage, and that infected $LMP7^{-/-}$ mice have less inflammatory cell recruitment to the heart compared to infected $LMP7^{+/+}$ mice. To determine whether these findings correlated with other measures of cardiac damage during acute infection, serum cTnI was measured at 9 dpi (Fig. 3G). There was an increase in the concentration of cTnI in the sera of infected mice compared to mock-infected mice. However, there were no differences in cTnI concentrations between $LMP7^{+/+}$, $LMP7^{+/-}$, and $LMP7^{-/-}$ mice at this time point.

Effect of Immunoproteasome Deficiency on Viral Replication

MAV-1 replicates in hearts following infection of 7-day-old mice. Because we saw some differences between $LMP7^{+/+}$, $LMP7^{+/-}$, and $LMP7^{-/-}$ mice in virus-induced inflammation, such as decreased expression of IL-1β, increased expression of CCL5, and less cardiac tissue damage in $LMP7^{-/-}$ mice, we subsequently determined whether those differences in host responses were correlated with corresponding differences in viral replication. MAV-1 DNA was readily detectable in the hearts of all infected mice at 9 dpi (Fig. 4). However, there was no statistically significant difference in viral loads between $LMP7^{+/+}$, $LMP7^{+/-}$, and $LMP7^{-/-}$ mice.

DISCUSSION

This study investigated the effects of IP deficiency on the pathogenesis of adenovirus myocarditis by studying an adenovirus in its natural host using MAV-1. MAV-1 infection of

neonates caused increased proinflammatory cytokine production and cardiac tissue damage. IP deficiency had variable effects on the production of different cytokines, but seemed to lessen the degree of overall cardiac inflammation following infection.

We looked at β1i and β2i to verify that there was no compensatory upregulation in the absence of β5i. If there were, and the result was corresponding compensatory IP activity, then that could explain the lack of an effect on cytokine expression, viral replication, and pathogenesis in LMP7$^{-/-}$ mice. The results confirmed that β1i and β2i were not upregulated in the absence of β5i. β1i and β2i actually followed a similar trend as β5i between the respective genotypes, with the lowest level of gene expression across infected groups in LMP7$^{-/-}$ mice. However, the differences in β1i and β2i gene expression between infected groups were not statistically significant, so the biological relevance of the trend is unclear. These results could suggest that without β5i, gene expression of β1i and β2i is also slightly decreased due to the fact that they need β5i in order to be incorporated into the IP. β1i and β2i overproduction would be inefficient without adequate β5i. Regardless of these individual measures, we have not quantified overall IP activity in this experiment.

We detected upregulation of multiple proinflammatory cytokines in the hearts of infected mice. This reflects what has been observed in a previous study of cytokine expression in the hearts of mice infected with MAV-1 (McCarthy et al., 2013). Although these cytokines play a protective role in viral myocarditis, their production has detrimental consequences by contributing to inflammatory tissue damage. Proper resolution of viral infection requires a delicate balance of the host immune response between a level that promotes viral clearance and one that minimizes detrimental effects on the host tissue. We sought to determine the effect of IP deficiency on the expression of proinflammatory cytokines to evaluate the extent to which IP activity contributed to virus-induced inflammation. Because

the IP contributes to inflammation and immune function in a variety of ways, we expected that less induction of many proinflammatory cytokines would be detected and that a corresponding decrease in host tissue damage in the absence of IP activity would be observed.

IFN-ɣ is induced during MAV-1 myocarditis, and depletion of IFN-ɣ during acute infection reduces cardiac inflammation in MAV-1-infected mice (McCarthy et al., 2015). In a different model, β1, β2, and β5 subunits are induced by both IFN-ɣ and TNF-α (Aki et al., 1994). Other work from our laboratory has shown that IP activity is absent in the hearts of IFN-ɣ-deficient mice, solidifying the link between IFN-ɣ and IP activity during MAV-1 myocarditis (Mary McCarthy, unpublished data). Because of these correlations, we investigated the effects of IP deficiency on virus-induced IFN-ɣ expression. Had there been decreased viral replication in LMP7$^{-/-}$ mice, leading to a corresponding decrease in virus induction of IFN-ɣ, β5i deficiency would have been expected. However, because there were no differences in viral replication between LMP7 genotypes, our results showed no significant effect of β5i deficiency on IFN-ɣ expression.

TNF-α is a cytokine produced by macrophages that is involved in systemic inflammation (Hallermalm et al., 2001). Previous studies have shown that TNF-α may act synergistically with IFN-ɣ to upregulate β5i expression, contributing to IP activation (Hallermalm et al., 2001). Through NF-κB activation, which plays a central role in the regulation of immunity and inflammation, IP activity may also influence TNF-α expression (reviewed in McCarthy et al., 2014). We addressed this with LMP7$^{-/-}$ mice, allowing us to indirectly examine the effects of IP activity on NF-κB activation through the evaluation of downstream NF-κB-mediated inflammatory responses. However, there were no significant differences between LMP7 genotypes in TNF-α gene expression in the heart following infection. IP activity, therefore, does not seem essential for TNF-α induction. This may be

because many other pathways converge on NF-κB signaling, so the absence of a single one (such as the IP) may not have a noticeable effect on TNF-α expression.

We did detect less expression of IL-1β in the hearts of infected LMP7$^{-/-}$ mice than LMP7$^{+/+}$ mice, suggesting that IP activity does contribute to some elements of the host response to MAV-1 infection. IL-1β is produced by activated macrophages and is an important mediator of the inflammatory response (Ren et al., 2009). It can contribute to cell proliferation, differentiation, and death by apoptosis (Ren et al., 2009). While IL-1β promotes viral clearance when expressed at a reasonable level, excessive production leads to host tissue damage. This suggests that suppression of IL-1β may actually be beneficial to the host, potentially decreasing tissue damage caused by excessive inflammation. The correlation between decreased IL-1β expression and fewer inflammatory cell infiltrates in the hearts of LMP7$^{-/-}$ mice suggests that IP inhibition has the potential to serve as a therapeutic strategy for patients with viral myocarditis.

CCL5 is a chemokine that is chemotactic for T cells, eosinophils, and basophils (Basler et al., 2013). This chemokine, along with CXCL1, is induced during MAV-1 infection (McCarthy et al., 2013). CCL5 recruits leukocytes to sites of inflammation and is involved in activating certain types of natural-killer (NK) cells to form CHAK (CC-Chemokine-activated killer) cells (Basler et al., 2013). We detected higher CCL5 expression in MAV-1 mice than in mock-infected mice. Furthermore, we observed that CCL5 was upregulated to a greater extent in LMP7$^{-/-}$ infected mice than in LMP7$^{+/+}$ infected mice. It seems possible that this is a compensatory response offsetting the reduced expression of other mediators. To limit pathological dysfunction, the immune system is capable of exerting compensatory immune suppression in the event of an inflammatory response (Xu et al., 2014). Likewise, due to the nature of the immune system and the complicated interactions that occur between various

elements of the immune response, increased expression of one cytokine to compensate for reduced expression of another is not entirely unexpected.

Histological evaluation of neonatal hearts suggested that MAV-1 infection caused less severe cardiac inflammation in mice lacking the β5i subunit than in mice that fully expressed it. This data, correlated with the reduced level of IL-1β in LMP7-deficient mice, suggest that a decrease in IP activity suppresses certain components of the immune system.

Although specific mechanisms regulating the effects of T cells in the heart during MAV-1 myocarditis have not yet been identified, it is thought that T cells contribute to both tissue damage and control of viral replication in the heart during acute MAV-1 infection (McCarthy et al., 2015). We have also observed higher viral loads during MAV-1 infection following the depletion of CD8 T cells (unpublished data). Our findings show that $CD3^+$ T cells were recruited to the hearts of neonatal mice after MAV-1 infection. This is consistent with observations that hearts of patients with HAdV myocarditis are infiltrated with T cells (Kühl et al., 2005). There was no difference in $CD3^+$ T cell recruitment between LMP7 genotypes. However, we can not exclude the possibility that there may be an effect on specific aspects of CD8 T cell function, which may be impacted by IP deficiency more so than recruitment. Even if these aspects were affected by IP deficiency, the results suggest that they don't seem to have a dramatic effect on MAV-1 replication. Similarly, although cTnI levels were higher in MAV-1-infected than mock-infected mice, there was no significant difference between LMP7 genotypes, suggesting that there were no significant differences in cardiac muscle cell death among the infected groups. We did see some effects on certain measures on inflammation, but no differences in tissue damage were observed. This suggests that maybe other aspects of inflammation may make more meaningful contributions to tissue damage. Another

possibility is that, unlike in other models of viral myocarditis, tissue damage is more dependent on viral replication than on inflammation.

Because viral pathogenesis involves both virus-induced inflammatory responses and viral replication, we measured heart viral loads to characterize the effects of IP deficiency on viral replication. Acting indirectly through the contribution of host responses important in controlling viral replication, the IP regulates CD8 T cell responses to many viral antigens during infection (McCarthy et al., 2015). Therefore, decreased or absent IP activity could lead to increased viral replication in the heart. There was no difference, however, in heart viral loads between the various LMP7 genotypes. This suggests that any histological differences observed in the absence of IP activity had emerged due to effects of host inflammatory responses, and not by differences in viral replication.

In summary, these findings demonstrate that IP deficiency does affect some, but not all, measures of virus-induced inflammation in the heart following MAV-1 infection. Some of our data, such as the measurement of IL-1β and histology, suggest that IP inhibition could decrease inflammation and potentially be beneficial to the host. Still, more work needs to be done in order to better define potential contributions of IP deficiency to patients suffering from myocarditis caused by adenoviruses and other pathogens. The MAV-1 model of adenovirus myocarditis will facilitate further investigation of adenovirus pathogenesis, including continued work to define the role of the IP in viral infection. Studies such as this one on the role of the IP in adenovirus infection have the potential to guide development of novel therapeutic strategies, ultimately offering better treatment options for viral myocarditis.

ACKNOWLEDGMENTS

I'd like to thank Dr. Jason Weinberg and the rest of the Weinberg laboratory for their nonstop encouragement, help, and support throughout my undergraduate career in the lab. Everything

I have learned about scientific research and being a part of a virology lab has come from them, and I greatly appreciate it. I also appreciate the time dedicated by Dr. Sharlene Day and Dr. Bethany Moore to being readers of my honors thesis. Finally, I'd like to thank my parents - without them, I wouldn't have been lucky enough to attend the University of Michigan, and I would have never been granted this amazing opportunity.

REFERENCES

1. Aki, M. Shimbara, N., Takashina, M., Akiyama, K., Kagawa, S., Tamura, T., Tanahashi, N., Yoshimura, T., Tanaka, K., and Ichihara, A. (1994). Interferon-gamma induces different subunit organizations and functional diversity of proteasomes. *J Biochem* 115, 257-269.

2. Amabile N, Fraisse A, Bouvenot J, Chetaille P, Ovaert C. (2006). Outcome of acute fulminant myocarditis in children. *Heart 92* 1269–1273.

3. Basler M., Kirk C. J., Groettrup M. (2013). The immunoproteasome in antigen processing and other immunological functions. Curr. Opin. *Immunol. 25* 74–80.

4. Bowles NE, Ni J, Kearney DL, Pauschinger M, Schultheiss H-P,McCarthy R, Hare J, Bricker JT, Bowles KR, Towbin JA. (2003). Detection of viruses in myocardial tissues by polymerase chain reaction. evidence of adenovirus as a common cause of myocarditis in children and adults. J Am Coll Cardiol 42:466–472.

5. Dinarello, CA. (2009). Immunological and inflammatory functions of the interleukin-1 family. *Annual Review of Immunology 27.* 519-550.

6. Griffin, T.A., Nandi, D., Cruz, M., Fehling, H.J., Kaer, L.V., Monaco, J.J., and Colbert, R.A. (1998). Immunoproteasome assembly: cooperative incorporation of 844 interferon gamma (IFN-gamma)-inducible subunits. J Exp Med 187, 97-104.

7. Groettrup M., Standera S., Stohwasser R., Kloetzel P. M. (1997). The subunits MECL-1 and LMP2 are mutually required for incorporation into the 20S proteasome. Proc. Natl. Acad. Sci. U.S.A. 94 8970–8975 10.1073/pnas.94.17.897.

8. Hallermalm, K., Seki, K., Wei, C., Castelli, C., Rivoltini, L., Kiessling, R., Levitskaya, J. (2001). Tumor necrosis factor-alpha induces coordinated changes in major histocompatibility class I presentation pathway, resulting in increased stability of class I complexes at the cell surface. *Blood 98*, 1108-1115.

9. Kühl U, Pauschinger M, Noutsias M, Seeberg B, Bock T, Lassner D, Poller W, Kandolf R, Schultheiss H-P. (2005). High prevalence of viral genomes and multiple viral infections in the myocardium of adults with “idiopathic” left ventricular dysfunction. Circulation 111:887–893.

10. McCarthy, M., Levine, R., Procario, M., McDonnell, P., Zhu L., Mancuso, P., Crofford, L., Aronoff, D., Weinberg, J. (2013). Prostaglandin E2 induction during mouse adenovirus type 1 respiratory infection regulates inflammatory mediator generation but does not affect viral pathogenesis. *PLoS One*.

11. McCarthy, M., Procario, M., Twisselmann, N., Wilkinson, JE., Archambeau, AJ., Michele, DE., Day, SM., Weinberg, JB. (2015). Proinflammatory effects of interferon gamma in mouse adenovirus 1 myocarditis. *Journal of Virology 89,* 468-479.

12. McCarthy, M., Weinberg, JB. (2014). The Immunoproteasome and Viral Infection: A Unique Regulator of Complex Immune Pathways. Review. *Frontiers in Microbiology.*

13. Rock K. L., Gramm C., Rothstein L., Clark K., Stein R., Dick L., et al. (1994). Inhibitors of the proteasome block the degradation of most cell proteins and the generation of peptides presented on MHC class I molecules. *Cell 78* 761–771.

14. Shin E. C., Seifert U., Kato T., Rice C. M., Feinstone S. M., Kloetzel P. M., et al. (2006). Virus-induced type I IFN stimulates generation of immunoproteasomes at the site of infection. *J. Clin. Invest.* 116 3006–3014.

15. Xu X, Qiu C, Zhu L, Huang J, Li L, Fu W, Zhang L, Wei J, Wang Y, Geng Y, Zhang X, Qiao W, Xu J (2014). IFN-stimulated gene LY6E in monocytes regulates the CD14/TLR4 pathway but inadequately restrains the hyperactivation of monocytes during chronic HIV-1 infection. J Immunol. *8* 4125-4146.

TABLE 1 Primers and probes used for real-time PCR analysis

Target	Oligonucleotide	Sequence (5’ to 3’)
MAV-1 E1A genomic	Forward primer	GCACTCCATGGCAGGATTCT
	Reverse primer	GGTCGAAGCAGACGGTTCTTC
	Probe	TACTGCCACTTCTGC
IFN-ɣ	Forward primer	AAAGAGATAATCTGGCTCTGC
	Reverse primer	GCTCTGAGACAATGAACGCT
TNF-α	Forward primer	CCACCACGCTCTTCTGTCTAC
	Reverse primer	AGGGTCTGGGCCATAGAACT
GAPDH	Forward primer	TGCACCACCAACTGCTTAG
	Reverse primer	GGATGCAGGGATGATGTTC
IL-6	Forward primer	CTGCAAGAGACTTCCATCCAG
	Reverse primer	AGTGGTATAGACAGGTCTGTTGG
IL-1β	Forward primer	GCAACTGTTCCTGAATCTAACT
	Reverse primer	ATCTTTTGGGGTCCGTCAACT
β1i	Forward primer	ATGGCAGTGGAGTTTGACGG
	Reverse primer	ATACCTGTCCCCCCTCACATTG
β2i	Forward primer	GCTTGTGTTCCGAGATGGAGTC
	Reverse primer	TCCGTTCAAATCAACCCCG
β5i	Forward primer	CATTCCTGAGGTCCTTTGGTGG
	Reverse primer	ATGCGTTCCCCATTCCGAAG

TABLE 2 Quantification of cellular inflammation in histological specimens

Score	Description
Severity*	
0	No inflammatory infiltrates
1	Inflammatory cells present without discrete foci
2	Larger foci of 10 to 100 inflammatory cells
3	Larger foci of >100 inflammatory cells
Extent	
1	Mild (<25% of section involved)
2	Moderate (~25-75% of section involved)
3	Severe (>75% of section involved)

*A score from 0 to 3 was given for the size/intensity of cellular infiltrates. The score was then multiplied by a number reflecting the extent of involvement in the specimen to reach a final severity score, resulting in a total score that could range from 0 to 9.

FIGURE 1 Immunoproteasome Subunit Expression in LMP7$^{-/-}$Mice

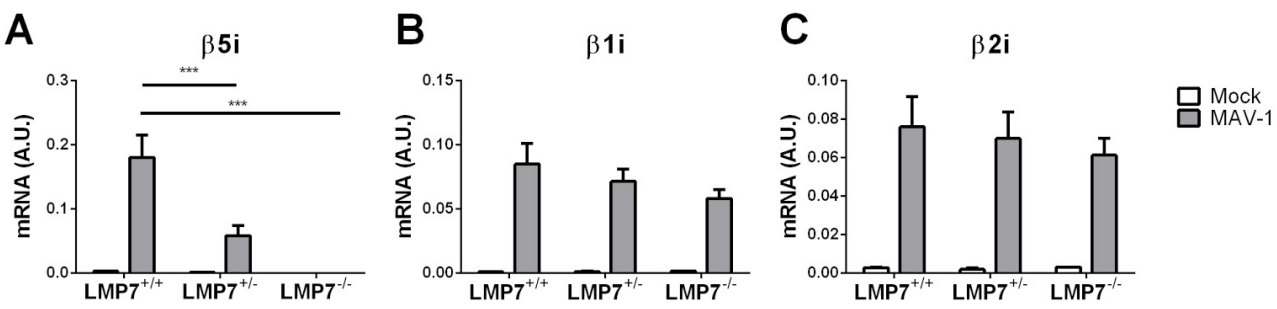

FIG 1 β5i in hearts at 9 dpi. Expression of the β5i (A), β1i (B), and β2i (C) genes in the heart were measured by RT-qPCR, shown in arbitrary units and standardized to GAPDH. Combined data from 6 to 8 mice per infected group and 1 to 3 mice per mock-infected group are presented as means ± SEM. ***, P < 0.001 (comparing MAV-1 LMP7$^{+/+}$ to MAV-1 LMP7$^{+/-}$ and LMP7$^{-/-}$ at 9 dpi).

FIGURE 2 Effect of Immunoproteasome Deficiency on Virus-Induced Inflammation

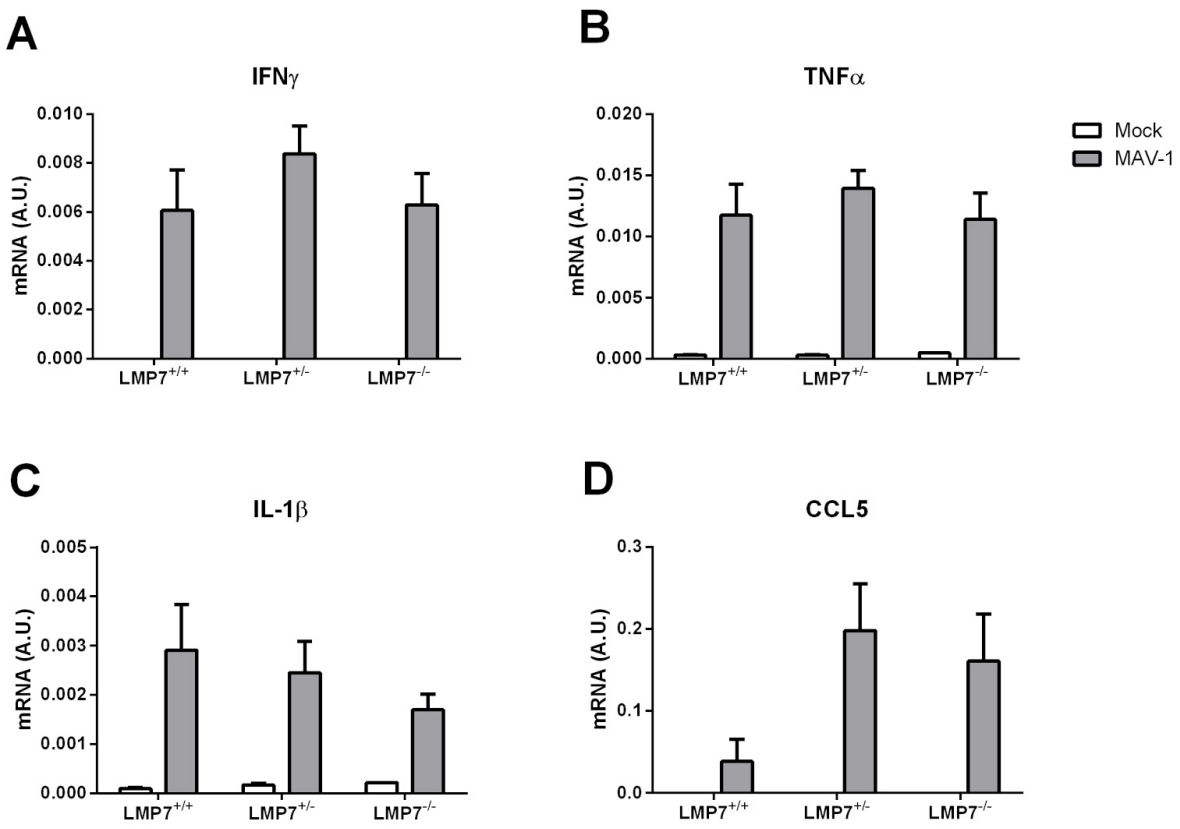

FIG 2 IFN-ɣ, TNF-α, IL-1β, and CCL5 in hearts at 9 dpi. Mice of different LMP7 genotypes were infected i.n. with MAV-1. Expression of IFN-ɣ (A), TNF-α (B), IL-1β (C), and CCL5 (D) genes in the heart were measured by RT-qPCR, shown in arbitrary units and standardized to GAPDH. Combined data from 6 to 8 mice per infected group and 1 to 4 mice per mock-infected group are presented as means ± SEM.

FIGURE 3 Effect of LMP7 Deficiency on Inflammatory Infiltrates in Infected Neonate Heart

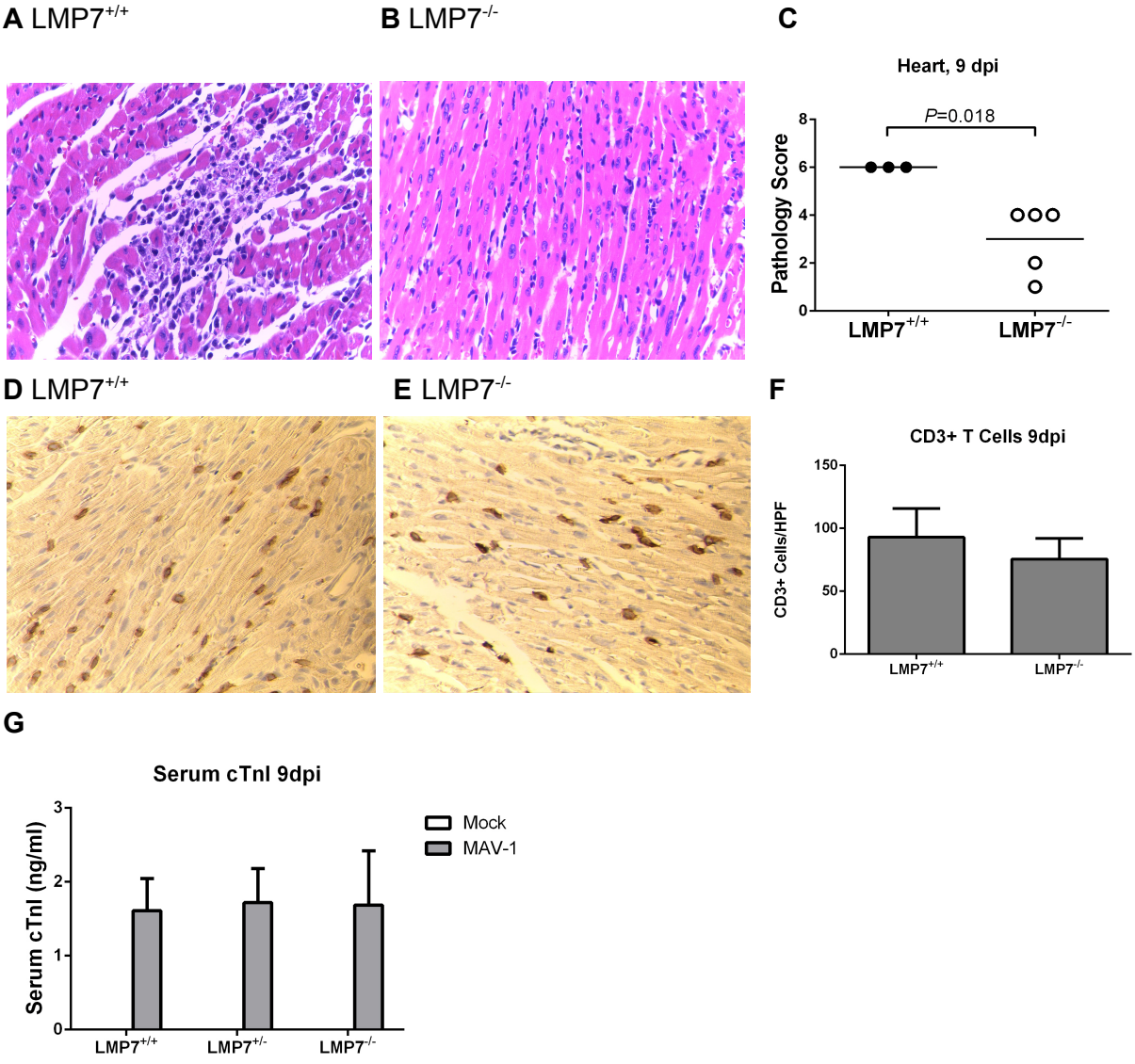

FIG 3 Inflammatory cell infiltrates in hearts of infected neonatal mice. Mice of different LMP7 genotypes were infected i.n. with MAV-1. (A,B) Hematoxylin and eosin-stained (H&E) sections and (D,E) CD3-stained sections were prepared from paraffin-embedded sections. Representative H&E-stained sections from hearts are shown at 25x magnification. (C) Pathology Scores assigned according to Table 2. Combined data from 1 to 5 mice per group are presented as means ± SEM. (F) CD3 staining was quantified by counting the number of $CD3^+$ cells per high-power field, averaging three fields per individual mouse. Combined data from 4 to 5 mice per infected group are presented as means ± SEM. (G) Serum cTnI levels were measured by ELISA. Combined data from 1 to 3 mice per mock-infected group and 3 to 5 mice per infected group are presented as means ± SEM.

FIGURE 4 Effect of Immunoproteasome Deficiency on Viral Replication

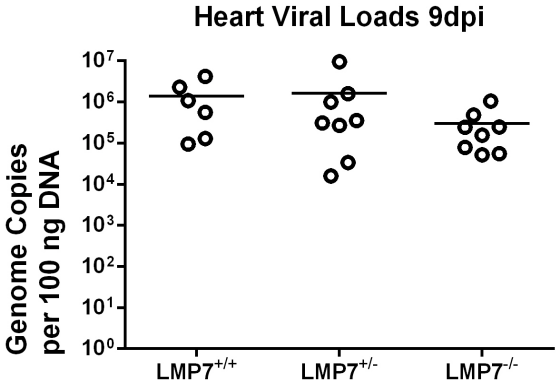

FIG 4 Viral loads in hearts of MAV-1 infected neonatal mice at 9 dpi. Mice of different LMP7 genotypes were infected i.n. with MAV-1. DNA was extracted from hearts of mice, and qPCR was used to quantify copies of MAV-1 genome. DNA viral loads are expressed as copies of MAV-1 genome per 100 ng of input DNA. Individual circles represent values for individual mice, and horizontal bars represent means for each group.